Appl. Phys. A (2015) 121:157–162
DOI 10.1007/s00339-015-9402-y

Applied Physics A
Materials Science & Processing

Simple fabrication of closed-packed IR microlens arrays on silicon by femtosecond laser wet etching

Xiangwei Meng[1] · Feng Chen[1] · Qing Yang[1] · Hao Bian[1] · Guangqing Du[1] · Xun Hou[1]

Received: 14 April 2015 / Accepted: 31 July 2015 / Published online: 12 August 2015

Abstract We demonstrate a simple route to fabricate closed-packed infrared (IR) silicon microlens arrays (MLAs) based on femtosecond laser irradiation assisted by wet etching method. The fabricated MLAs show high fill factor, smooth surface and good uniformity. They can be used as optical devices for IR applications. The exposure and etching parameters are optimized to obtain reproducible microlens with hexagonal and rectangular arrangements. The surface roughness of the concave MLAs is only 56 nm. This presented method is a maskless process and can flexibly change the size, shape and the fill factor of the MLAs by controlling the experimental parameters. The concave MLAs on silicon can work in IR region and can be used for IR sensors and imaging applications.

1 Introduction

Microlens arrays (MLAs) are important integrated optical components for optical systems, micro-manufacturing and biochemical systems [1–3]. Recently, microlenses made of silicon were successfully developed for infrared (IR) charge-coupled device (CCD) and IR sensor [4–6]. The silicon MLAs are ideal IR optical devices to improve the performance of IR detector, which is strongly desired to integrate into the IR microsensors and IR imaging microsystems [7, 8]. MLAs with high fill factor can capture more incident lights, increasing the collection efficiency and the signal-to-noise ratio [9–11]. Therefore, the silicon MLAs with high fill factor are continuously pursued.

However, fabrication of closed-packed MLAs on silicon is still challenging for most current processing methods. Generally, several techniques for the fabrication of concave MLAs have been proposed. The concave profiles on Si are fabricated by an inductively coupled plasma (ICP) etcher for masked and maskless etching method [12]. The resist lithography is used in the masked etching step. A similar method of protecting the substrate with a hard mask and isotropic wet etching was used to fabricate concave microstructure on Si [13]. Here, the thermal oxide (SiO_2) and silicon nitride (Si_3N_4) layer was used as the mask with isotropic wet etching of Si in the solutions containing a mixture of hydrofluoric acid (HF) and nitric acid (HNO_3). The electrochemical anodization in HF electrolyte was used to substitute the mixture of HF and HNO_3 as etching solution [14]. The spherical and cylindrical concave micromirrors in Si are fabricated as distributed Bragg reflectors. The small sub-micron apertures are induced by the femtosecond laser on the hard mask films with minimal collateral damage on the Si substrates, so the inverted pyramid microstructures are formed by anisotropic etching. However, it is difficult to fabricate the high fill factor MLAs, and these methods require expensive equipments and complicated procedures to create the resist coating film or hardmask on the substrates. These photomasks should be pre-designed, and the shapes of the concave microstructures are not flexibly controlled [15, 16].

We have successfully prepared MLAs on the K9 glass based on femtosecond laser irradiation assisted by wet etching (FLIWE) method [17, 18]. In this work, we perform a simple, high-efficient maskless technique to fabricate concave silicon MLAs with high fill factor for

✉ Feng Chen
chenfeng@mail.xjtu.edu.cn

[1] State Key Laboratory for Manufacturing System Engineering and Key Laboratory of Photonics Technology for Information of Shaanxi Province, School of Electronics and Information Engineering, Xi'an Jiaotong University, Xi'an 710049, People's Republic of China

enhancing the detectivity of IR detector. In the laser irradiation process, amorphization, annealing and ablation occurred, and then the heat-affected regions of damaged amorphous and microstructures are observed on the laser focused spots [19]. In the wet etching process, the induced region has a higher selective etch rate than the un-irradiated regions and the ablation craters can gradually spread. With the increase in etching time, the size of the craters increases and the surface becomes smooth. Finally, the adjacent concave microstructures would meet and overlap with each other. Then, the concave MLAs with high fill factor were formed by this maskless method. This work is shown as a novel method to fabricate the MLAs on the silicon, which are highly desired in the IR region for sensors and micro-optical systems. The fabricated MLAs are also used as molds to replicate convex MLAs on polymers [20].

2 Fabrication process

The fabrication process of the MLAs is shown in Fig. 1. A femtosecond Ti:sapphire laser system (Coherent Libra-usphe, pulse duration 50 fs, central wavelength 800 nm, repetition rate 1 kHz) was used in the experiment (Fig. 1a). The laser power and the number of irradiation pulses were controlled by a variable attenuator and a fast mechanical shutter, respectively. The laser beam was focused on the surface of silicon by an objective lens (NA = 0.50, Olympus). The optical setup was similar to [17]. After the laser irradiations, we optimized a mixture solution of HF, nitric acid (HNO_3) and acetic acid (CH3COOH), i.e., HNA in proportion 6:10:9 to remove the modified materials at room temperature (23 °C). The concentrations of HF, HNO_3 and CH_3COOH are 40, 60 and ≥99.5 %, respectively. The isotropic etching of silicon in the mixture was a standard technique in microelectromechanical system (MEMS) micromachining. HNO_3 created an oxide layer at the silicon surface that can be subsequently etched away by HF. In the mixed acid, the laser-modified materials have much higher selective etching rate than the un-irradiation regions. The isotropic chemical etching occurs in the laser-irradiated spots and results in the circular-shaped concave structures in rectangular or hexagonal arrangement. The circular-shaped concave structures became smooth and expanded gradually until the adjacent ones overlapped with each other. The shape of microlenses formed rectangles or hexagons and filled the surface completely. Then, the concave MLAs with high fill factor were formed and they were washed in deionized water. Using the concave MLAs as mold, corresponding convex MLAs were obtained on poly (dimethyl siloxane) (PDMS) film by the replica molding process.

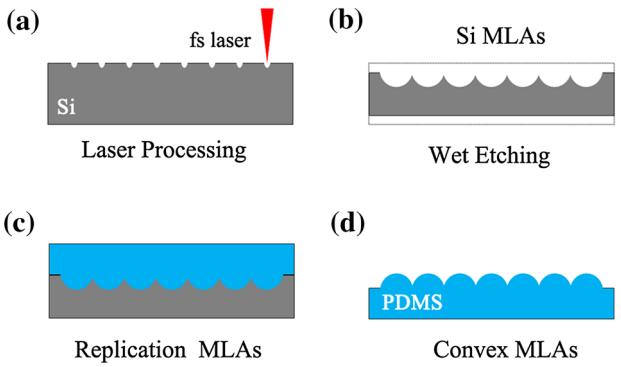

Fig. 1 Schematic diagram of the fabrication process. **a** An array of laser-exposed spots is produced on silicon wafer by laser irradiation. **b** Concave microstructures with smooth surfaces are formed by chemical wet etching process. **c** The replication procedure. **d** Convex PDMS MLAs

3 Results and discussion

Figure 2 shows the scanning electron microscope (SEM) images of the concave MLAs and demonstrates the ability to fabricate smooth surface and uniform MLAs by this method. In the laser irradiation process, every spot was induced by 400 femtosecond laser pulses with the laser power of 3 mW. In the etchant, the modified materials were rapidly dissolved by the isotropic etching process in 3 min. The chemical polishing was done at the same time. The diameter and depth of the concave microlens are increasing and the surface roughness decreasing until the modified materials are completely removed. The isotropic or anisotropic etching of Si with hard mask to fabricate microstructures was studied by Albero et al. and Kumar et al. [13, 15, 21]. In our experiment, we obtained similar microstructure without the hard mask. The FLIWE method is widely used to fabricate the 2D and 3D microstructures in our group [17, 18, 22]. The shape of the MLA can be controlled by the pre-designed arrangement of the laser focus spots. When the focus spots were arranged with hexagonal arrangement, the hexagonal MLAs were fabricated by the wet chemical etching, as shown in Fig. 2a, c. In the same way, the MLAs with rectangular arrangement were also fabricated, as shown in Fig. 2b, d. The fill factor of MLAs is a key condition that impacts the overall light efficiency. The MLAs with high fill factor can capture more incident lights to keep the high signal-to-noise ratio and improve the performance of the devices, so the closed-packed MLAs are pursued in micro-optical system. In the etching process, the concave microstructures expanded and the etching process did not stop until the adjacent microstructures overlapped with each other. Hence, the fill

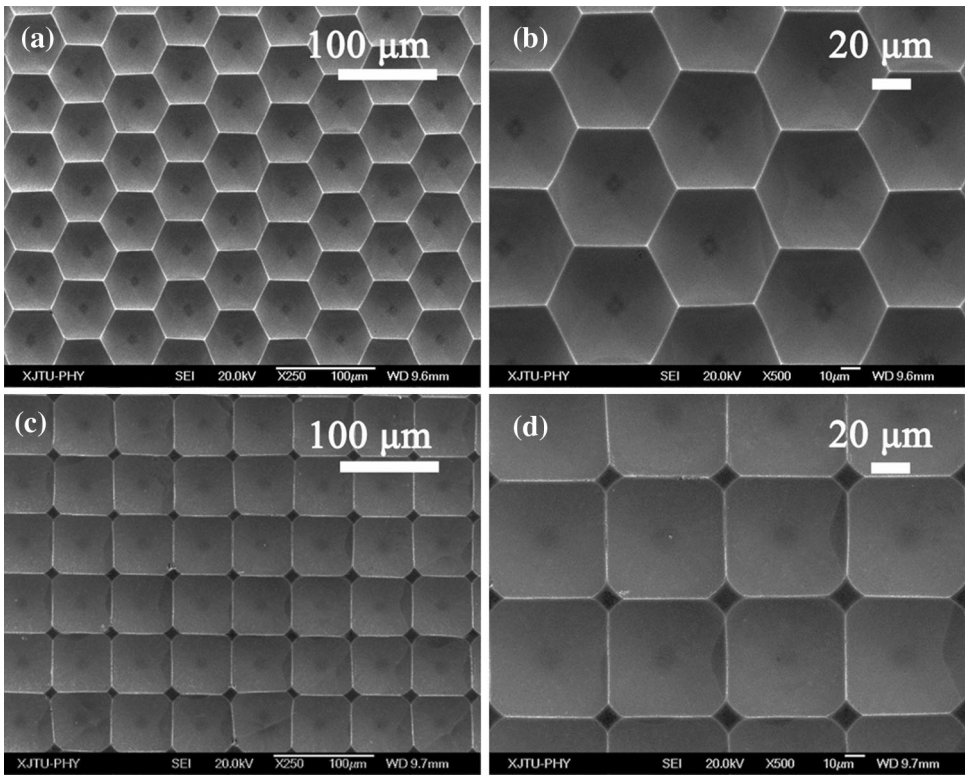

Fig. 2 SEM images of (**a**) (**b**) the hexagonal microlens array and (**c**) (**d**) the rectangular microlens array

factor of the concave MLAs is close to 100 %, and the results are better than that of Pan et al. [23]. The diameter of the 100 % fill factor MLAs is decided by the distance of the adjacent spots and their arrangement [24]. MLAs with other patterns can be also realized using the method described in Ref. [18]. In the laser irradiation process, the position of every laser ablation point can be located precisely, so the arrangements of MLAs can be flexibly designed by the computer program. The results demonstrate that our method can get MLAs with different shapes to satisfy various specific IR applications in the micro-optical systems [24].

The 3D and cross-section profiles of the MLA are measured by a laser scanning confocal microscope (LSCM, Olympus LEXT OLS4000), as shown in Fig. 3. The gapless concave MLAs with hexagonal arrangement are shown in Fig. 3a. The aperture diameter, D, and the sag height, h, of the hexagonal MLA are also measured in Fig. 3c, and the values are 59.74 and 15.4 μm, respectively. Figure 3b and d shows the measured results of the rectangular MLAs, and the value is 59.32 μm in diameter and its sag height is 13.38 μm. The roughness of the MLAs, Ra, is also measured in an area of 128 × 128 μm^2 for rectangular MLAs, and the result is 56 nm.

As shown in Fig. 4a, the measured profiles of the hexagonal MLAs and the fit of the parabolic profile are compared. The profile of the MLAs fits very well with the parabolic surface. As mentioned above, the etching time is a limit parameter for the diameter of MLAs. The diameter is measured at different etching times during the wet etching process, and the result is shown in Fig. 4b. The diameter is almost increasing linearly with the etching time. Therefore, the diameter can be controlled by adjusting the etching time.

To characterize the optical performance of the MLAs, we used a blue LED light to vertically irradiate the MLAs and capture the focal spots generated through the MLAs by an objective lens (Nikon, NA = 0.15) and a CCD, as shown in Fig. 5a. Through the reflection of the light by the rectangular and hexagonal MLAs, the microscope images of the focal spots are shown in Fig. 5b, c, respectively. The images reveal the uniformity of the irradiance distribution in the focal spots of MLAs. To prove the homogeneity of the focal spots, the focal spots intensity profile of the rectangular MLAs is presented, as shown in Fig. 5d. The deviation of the middle six focal spots intensity profile is small and is mainly caused by the light source. Figure 5 shows the good optical performance of the MLAs.

The concave MLAs could be used as a mold to replicate the convex MLAs on the polymer. In this work, the convex MLAs were fabricated on PDMS film by a replica molding process. The top view of the replicated MLAs is measured by an optical microscope (OM), as shown in Fig. 6a. The optical performance of the replicated MLAs is also studied

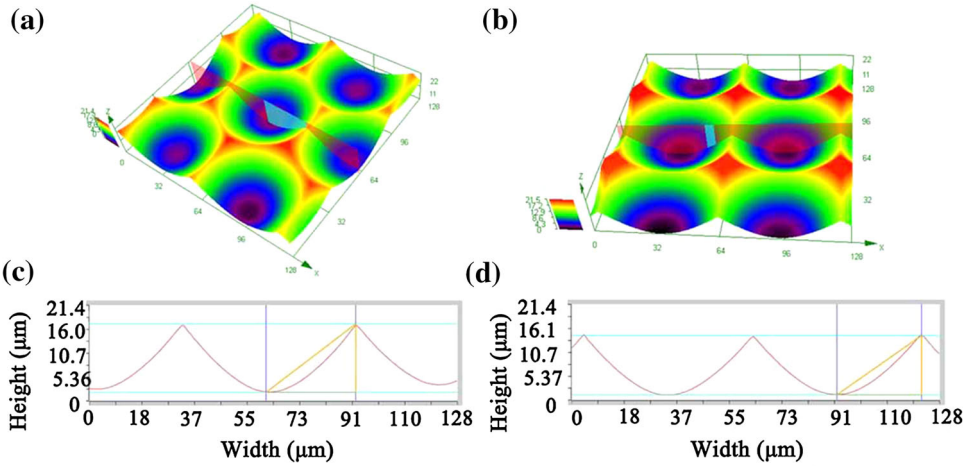

Fig. 3 Three-dimensional measurements of the MLAs. **a**, **c** The cross section and the 3D profiles of the hexagonal MLAs. **b**, **d** The cross section and the 3D profiles of the rectangular MLAs

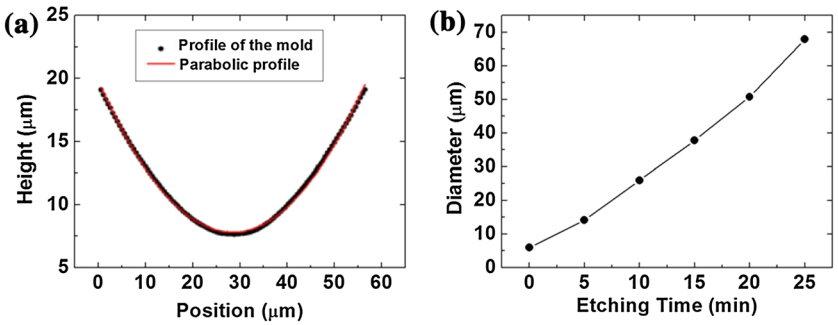

Fig. 4 **a** Measured profile of the MLAs and the fit of the parabolic profile. **b** The evolution of the diameter of the structures versus the wet etching time

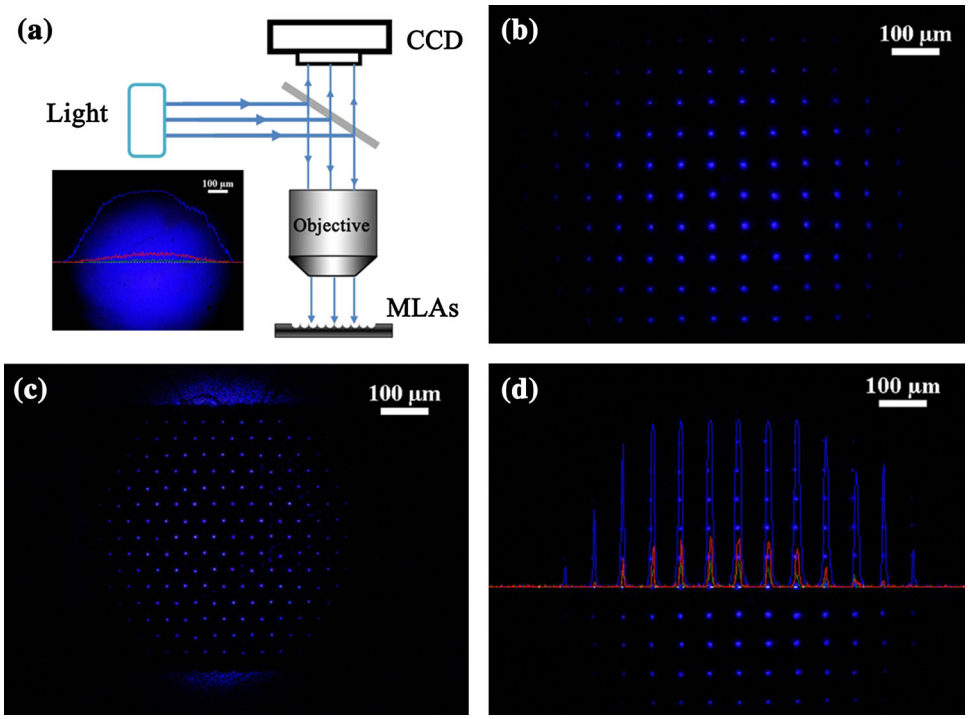

Fig. 5 Optical performance of the MLAs. **a** Schematic of the optical experimental setup. **b** The focal spots image of the rectangular MLAs. **c** The focal spots image of the hexagonal MLAs. **d** The distribution of the intensity profile

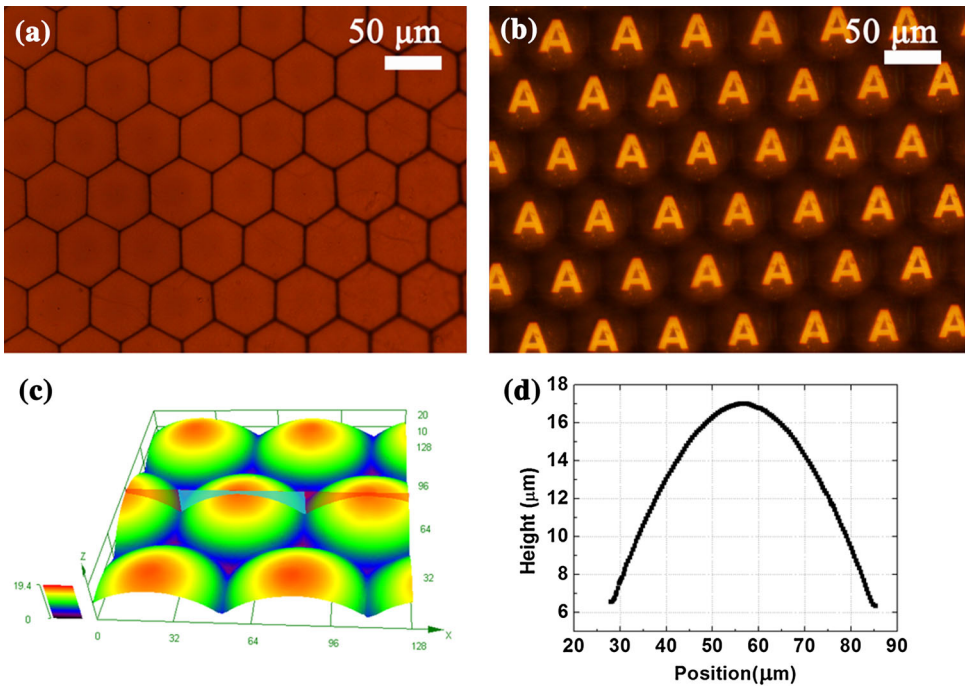

Fig. 6 Replication of the convex MLAs. **a** The optical microscope of the hexagonal MLAs. **b** The optical performance of the hexagonal MLAs. **c**, **d** The cross section and the 3D profiles of the hexagonal arrangement MLAs

by the optical microscope system, and the image is captured that appeared the high-quality imaging ability of the MLAs, as shown in Fig. 6b. The setup of imaging performance is similar to [17]. The 3D morphology and the cross-section profiles of convex MLAs are measured by LCSM, and the results are shown in Fig. 6c, d. The diameter and the height of the convex MLA are 57.20 and 11.29 μm, respectively. The curvature radius of the MLAs, R, can be estimated by the equation:

$$R = \frac{h^2 + r^2}{2h}, \tag{1}$$

where h is the height, r is the radius of the MLAs [17]. The value of the curvature radius, R, is 41.87 μm. The focal length of MLAs is often described by the formula

$$f = \frac{R}{n-1}, \tag{2}$$

where n is the refractive index of the PDMS ($n = 1.41$), and the focal length, f, is 102.12 μm. Furthermore, the numerical aperture, NA, of the MLAs is defined as

$$\mathrm{NA} = \frac{D}{2f}, \tag{3}$$

where D is the diameter of the MLAs, and the result of NA is 0.28. The height has been controlled by adjusting the scanning depth of the craters, as shown in Ref. [25]. So the NA of the MLAs can be also flexibly controlled.

4 Conclusions

We have presented a flexible method to fabricate the concave MLAs with 100 % fill factor on the silicon wafers. The high surface quality, high uniform and high optical performance of the MLAs are also demonstrated. By controlling the arrangements of the exposure spots, concave MLAs with different arrangements are achieved. Compared to the traditional lithography technology, our method is maskless and low-cost. This work provides a potential route to realize silicon MLAs and would be beneficial to developing the IR region applications in the microsensors and micro-optical systems. The fabricated concave molds with hexagonal-shaped structures are also used to replicate convex MLAs on PDMS.

Acknowledgments This work is supported by the National Science Foundation of China under the Grant Nos. 51335008, 61275008 and 61176113, the Special-funded program on National Key Scientific Instruments and Equipment Development of China under the Grant No. 2012YQ12004706.

References

1. S.I. Chang, J.B. Yoon, H. Kim, J.J. Kim, B.K. Lee, D.H. Shin, Opt. Lett. **31**, 3016–3018 (2006)
2. F. Merenda, J. Rohner, J.M. Fournier, R.P. Salathé, Opt. Express **15**, 6075–6086 (2007)
3. D. Wu, Q.D. Chen, L.G. Niu, J.N. Wang, J. Wang, R. Wang et al., Lab Chip **9**, 2391–2394 (2009)

4. K. Petroz, E. Ollier, H. Grateau, P. Mottier, Sens. Actuators, A **73**, 117–121 (1999)
5. C.F. Chen, S.D. Tzeng, H.Y. Chen, S. Gwo, Opt. Lett. **30**, 652–654 (2005)
6. C.J. Ke, X.J. Yi, J.J. Lai, S.H. Chen, Int. J. Infrared Millimeter Waves **26**, 133–146 (2005)
7. D.C. Appleyard, M.J. Lang, Lab Chip **7**, 1837–1840 (2007)
8. M. He, X.C. Yuan, K.J. Moh, J. Bu, X.J. Yi, Opt. Eng. **43**, 2589–2594 (2004)
9. H. Kwon, Y. Yee, C.H. Jeong, H.J. Nam, J.U. Bu, J. Micromech. Microeng. **18**, 065003 (2008)
10. H. Yang, C.K. Chao, M.K. Wei, C.P. Lin, J. Micromech. Microeng. **14**, 1197 (2004)
11. S.I. Chang, J.B. Yoon, Opt. Express **12**, 6366–6371 (2004)
12. K.P. Larsen, J.T. Ravnkilde, O. Hansen, J. Micromech. Microeng. **15**, 873–882 (2005)
13. J. Albero, L. Nieradko, C. Gorecki, H. Ottevaere, V. Gomez, H. Thienpont et al., Opt. Express **17**, 6283–6292 (2009)
14. Y.S. Ow, M.B.H. Breese, S. Azimi, Opt. Express **18**, 14511–14518 (2010)
15. K. Kumar, K.K.C. Lee, P.R. Herman, J. Nogami, N. P. Kherani, Appl. Phys. Lett. **101**, 222106 (2012)
16. K. Kumar, K.K. Lee, J. Nogami, P.R. Herman, N.P. Kherani, EPJ Photovolt. **4**, 45101 (2013)
17. F. Chen, H.W. Liu, Q. Yang, X.H. Wang, C. Hou, H. Bian et al., Opt. Express **18**, 20334–20343 (2010)
18. B. Hao, H. Liu, F. Chen, Q. Yang, P. Qu, G. Du et al., Opt. Express **20**, 12939–12948 (2012)
19. J. Bonse, S. Baudach, J. Krüger, W. Kautek, M. Lenzner, Appl. Phys. A **74**, 19–25 (2012)
20. Y. Hu, Q. Yang, F. Chen, H. Bian, Z. Deng, G. Du et al., Appl. Surf. Sci. **292**, 285–290 (2014)
21. J. Albero, C. Gorecki, L. Nieradko, B. Paivanranta, V. Gomez, H. Thienpont et al., J. Eur. Opt. Soc. Rapid Publ. **5**, 10001 (2010)
22. S. He, F. Chen, K. Liu, Q. Yang, H. Liu, H. Bian et al., Opt. Lett. **37**, 3825–3827 (2012)
23. A. Pan, B. Gao, T. Chen, J. Si, C. Li, F. Chen et al., Opt. Express **22**, 15245–15250 (2014)
24. C.T. Pan, C. Su, Sens. Actuators, A **134**, 631–640 (2007)
25. X.W. Meng, F. Chen, Q. Yang, H. Bian, H.W. Liu, P.B. Qu et al., IEEE Photonics Tech. Lett. **25**, 1336–1339 (2013)